Surface polaritons on generalized quasiperiodic gratings

J. Milton Pereira, Jr.,[1] E. L. Albuquerque,[2] G. A. Farias,[1] and R. N. Costa Filho[1]
[1]*Departamento de Física, Universidade Federal do Ceará, Campus do Pici, Caixa Postal 6030, 60451-970 Fortaleza-CE, Brazil*
[2]*Departamento de Física, Universidade Federal do Rio Grande do Norte, 59072-970 Natal-RN, Brazil*
(Received 20 September 2004; revised manuscript received 10 March 2005; published 15 July 2005)

In this work we calculate the spectrum of surface plasmon polaritons propagating on a medium with a surface described by a generalized quasiperiodic function. The profile function is defined in terms of unit cells containing binary elements, corresponding to elevations of different shapes, arranged according to an inflation rule that generates a quasiperiodic sequence. Our theoretical model, based upon a well-known formalism that has been applied to periodic surfaces, generalizes a previous calculation performed for the nonretarded limit. Numerical results show the effect of the quasiperiodicity on the dispersion relations and on the density of surface polaritons modes propagating on a semi-infinite free-electron metal.

DOI: 10.1103/PhysRevB.72.045433 PACS number(s): 73.20.Mf, 71.45.Gm

I. INTRODUCTION

Recently there has been a revival in the development of new techniques for the patterning of surfaces waves from both the theoretical and experimental point of view. Investigations in the search for photonic band gap materials[1] as well as quasiperiodic photonic crystal point defect laser[2] have led to a growing interest in the properties of electromagnetic surface modes on corrugated interfaces, not only due to the fundamental physical concepts employed to describe their intrinsic properties, but also for their potential device applications.[3] Among these modes, surface plasmon-polaritons (SPPs) play an important role in effects such as the extraordinary light transmission of surfaces with subwavelength holes[4] and the beaming effect of a single subwavelength slit surrounded by grooves.[5] Recently, a model of radiating light-surface plasmon coupling was developed allowing the extension of steady-state calculations, involving time independent incident and reflected intensities, to nonsteady-state situations, involving no incident light but exponentially time-dependent decaying emission intensity.[6]

Surface plasmon polaritons are collective Bloch modes that can be described as surface localized electromagnetic waves that propagate along a metal-dielectric interface (for a recent review, see Ref. 7). Due to their surface nature, the excitation of SPP modes by incoming electromagnetic waves is strongly influenced by the shape of the medium along which they propagate. Studies of SPP modes on randomly rough surfaces have shown the existence of localization effects[8] and the presence of absolute band gaps in their frequency spectrum.[9] Recent experimental results have also indicated the existence of SPP band gaps in media with periodic surface features.[10] The presence of defects, such as grooves or ridges, on an otherwise flat surface, can also lead to a large enhancement of the transmission of the electromagnetic fields at their vicinities, confirming the role of resonant tunneling processes involving states of the surface polariton Bloch modes. Furthermore, they are related to effects such as the surface enhanced Raman scattering[11] and surface enhanced second harmonic generation.[12]

Inspired by these theoretical and experimental results, Pereira *et al.* have recently developed a formalism for the calculation of the spectra of non-retarded surface-plasmons in quasiperiodic surfaces.[13] Quasiperiodic systems, which can be idealized as the experimental realization of a one-dimensional quasicrystal, have recently attracted a great deal of attention, especially due to the fact that they display properties observed neither in periodic nor in random systems. Also, they exhibit collective properties not shared by their constituent parts. The long-range correlations induced by the construction of these systems are expected to be reflected to some degree in their various spectra (as in light propagation, electronic transmission, density of states, polaritons, etc.), which are Cantor-like with critical eigenfunctions, defining a novel description of disorder. Indeed, theoretical transfer matrix treatments show that these spectra are fractals, which can be considered as their basic signature (for a review see Ref. 14).

Artificial quasiperiodic structures have been fabricated as MBE-grown multilayers.[15] It involves defining two distinct building blocks, each of them carrying out the necessary physical information, and having them ordered in a desired manner (for instance, they can be described in terms of a series of generations that obey a particular recursion relation). Furthermore, they have well-defined long-range positional order, such that their Fourier spectra contain δ peaks. Unlike in periodic crystals, these peaks should lie at all possible integer combinations of at least two intervals whose ratio is irrational.

In contrast with previous models, the quasiperiodic structure proposed in Ref. 13 is a pattern on the interface of a dielectric and the vacuum, with the elements of the unit cells being associated with well defined surface textures. Therefore, the quasiperiodic aspect of that system reflects a purely geometric property of the medium, which can in fact be described as being an intermediate state between a periodic grating and a randomly rough surface. In analogy to the multilayer structures, the surface profile is constructed in terms of deterministic quasiperiodic binary strings. The spectrum of nonretarded surface plasmons supported by the active medium was then shown to exhibit the characteristic fractal aspect, with the appearance of several frequency gaps as well as surface plasmon bands as the surface profile approached an actual quasiperiodic shape.

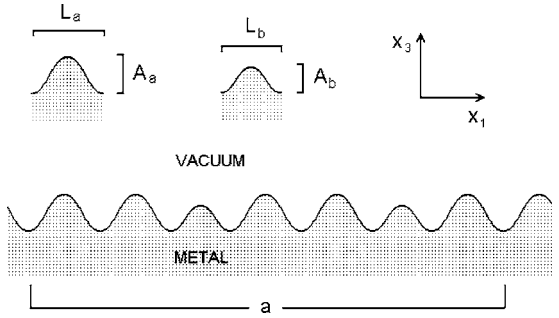

FIG. 1. Schematic representation of the surface profile, showing the two different types of ridges considered in this work. Here a is the size of the quasiperiodic unit cell.

In this paper we extend the formalism presented in Ref. 13 to obtain the spectra of surface plasmon polaritons in the retarded as well as in the nonretarded regimes, taking into account quasiperiodic surfaces. As in the previous calculation, the surface profiles are obtained in terms of unit cells, in which a set of parallel ridges are laid, and the shape of the unit cell is repeated on the surface along a direction perpendicular to the ridges. The unit cells considered here correspond to terms of quasiperiodic sequences that generalize the Fibonacci rule. Multilayer systems created according to these generalized Fibonacci sequences have been the subject of recent studies and were shown to display properties that are quite distinct from those created following the ordinary "golden-mean" Fibonacci sequence.[16] In order to calculate the SPP dispersion relation, we utilize an integral formalism based upon an approach that has been extensively applied previously to the study of the propagation of SPP in periodic dielectric surfaces.

The paper is structured as follows. In Sec. II a description is made about the surface model and the generalized quasiperiodic sequences are discussed. Section III gives a brief account of the theoretical method for calculating the dispersion relations of the SPP modes. In Sec. IV the results for the dispersion relations of the SPP modes are presented, along with results for the integrated density of modes. Finally, in Sec. V the results are summarized and conclusions are presented.

II. MODEL

The system consists of a semi-infinite dielectric medium with real permittivity, in which the dielectric-vacuum interface has a shape determined by a profile function $\zeta(x_1)$. The system profile is such that the region $x_3 < \zeta(x_1)$ is filled by the dielectric medium, whereas for $x_3 > \zeta(x_1)$ there is vacuum. Figure 1 depicts the schematic representation of the surface profile used in this work. The quasiperiodic surface is obtained by defining the $\zeta(x_1)$ function so that it has a quasiperiodic behavior. The surface actually has a periodic character in the sense that the quasiperiodic aspect is encoded in the definition of the unit cell itself. Specifically, in the present model the unit cell is defined to contain a set of ridges on an otherwise flat surface. The ridges can assume two different shapes and are aligned parallel to the x_1 direction. The positions of the different ridges correspond to the positions of the binary elements of a string from a quasiperiodic sequence. For each successive term of the sequences the period length a of the cell increases, and an actual quasiperiodic surface is obtained as the length of the unit cell grows to infinity.

The quasiperiodic sequences considered here are obtained by the recursive rule $(n \geqslant 1)$

$$S_{n+1} = S_n^p S_{n-1}^q, \tag{1}$$

where $S_0 = B$, $S_1 = A$ and p and q are positive integers denoting the number of adjacent repetitions of a given string, i.e., S_n^p represents p adjacent repetitions of the stack S_n. This type of inheritance is normal in iterative processes and frequently produces self-similar structures that are the basis of fractal configurations. When $p=q=1$ we have the well-known ordinary "golden-mean" Fibonacci sequence.

The strings can be generated in an equivalent way using the inflation rule

$$B \to A, \quad A \to A^p B^q. \tag{2}$$

The total number of elements A and B in each sequence is equal to the generalized Fibonacci number F_n, which is given by the recurrence formula

$$F_{n+1} = pF_n + qF_{n-1}, \tag{3}$$

with $F_0 = F_1 = 1$. In the limit $n \to \infty$ the ratio F_n/F_{n-1} approaches a characteristic number $\sigma(p,q)$ given by

$$\sigma = \frac{p \pm \sqrt{p^2 + 4q}}{2}. \tag{4}$$

For $p=q=1$, the first four terms in the sequence are $S_0 = B$, $S_1 = A$, $S_2 = AB$, and $S_3 = ABA$. In this case we find $\sigma(1,1) = (1+\sqrt{5})/2$, which is the well known golden mean. For $p = 2$, $q=1$ we have $S_2 = AAB$, $S_3 = AABAABA$, and $\sigma(2,1) = 1 + \sqrt{2}$ defines the so-called silver mean. For $p=3$, $q=1$ we have the the bronze mean $\sigma(3,1) = (9+\sqrt{13})/2$ with $S_2 = AAAB$, $S_3 = AAABAAABAAABA$. For $p=1$, $q=3$ we have the nickel mean $\sigma(1,3) = (1+\sqrt{13})/2$, with $S_2 = ABBB$ and $S_3 = ABBBA$. Observe that σ is completely equivalent to the determination of the eigenvalues of the substitution matrix R_ρ considered by Grimm and Baake.[17] Therefore, following the criteria defined in that reference, we can classify the substitution sequence considered in this paper based on the irrationality of $\sigma^-(p,q)$ [where the minus signal means the negative root of Eq. (4)], i.e., if $|\sigma^-(p,q)| < 1$, it is a Pisot-Vijayraghavan (PV) irrational number, and the fluctuation of the physical properties of the substitution sequence is more accentuated. On the other hand, if $|\sigma^-(p,q)| > 1$, it is not a PV-type number, and the fluctuation of its physical properties is minor.

As it was done in Ref. 13, the quasiperiodic sequence elements correspond to two types of ridges, labeled A and B, with heights A_a and A_b and widths L_a and L_b (see Fig. 1). The ridges are also chosen to be described by the sinusoidal functions

$$\zeta_a(x_1) = 2A_a \cos^2(\pi x_1/L_a), \tag{5}$$

in intervals $s_aL_a+s_bL_b-L_a/2<x<s_aL_a+s_bL_b+L_a/2$, for type A ridges, and

$$\zeta_b(x_1) = 2A_b \cos^2(\pi x_1/L_b), \tag{6}$$

in intervals $s_aL_a+s_bL_b-L_b/2<x<s_aL_a+s_bL_b+L_b/2$, for ridges of the B type, with $s_{a,b}=0,1,2,\ldots$ These functions were chosen since they allow us to obtain a continuous surface that approaches the well known sinusoidal grating profile with amplitude equal to $A_a/2$ as $A_b \to A_a$ and $L_b \to L_a$. The unit cell can be modeled by making a correspondence between the intervals assigned to each type of ridge and the elements of a binary string (see Fig. 1). The total length of the unit cell is then given by the sum of the widths of the ridges that it contains, and grows as the length of the strings that define it. An actual quasiperiodic surface is obtained as the length grows to infinity. For simplicity, throughout this paper we consider profiles with ridges of different heights, but with the same width (L).

III. THEORY

In order to calculate the SPP spectrum, we apply the integral formalism developed by Laks *et al.*,[18] based on the Rayleigh hypothesis, which has been widely used to investigate the propagation of SPP modes on weakly corrugated surfaces (i.e., height to width ratios <0.1) defined by analytic functions.[19–22] In this method, the magnetic field in the vacuum $\vec{H}^{>}(x_1,x_3,\omega)$, for $x_3>\zeta_{\max}$ and in the active medium region, $\vec{H}^{<}(x_1,x_3,\omega)$, for $x_3<\zeta_{\min}$ are written down, with $\zeta_{\min}$ and $\zeta_{\max}$ being the minimum and maximum values of $\zeta(x_1)$, respectively, with the assumption that they shall vanish as the distance $|x_3|$ from the interface increases. Then, by using Rayleigh's hypothesis, i.e., by extending the expressions for the fields to the region $\zeta_{\min}<x_3<\zeta_{\max}$, it is possible to express the boundary conditions for the tangent components of the fields at the interface $x_3=\zeta(x_1)$ as

$$H_2^{>}(x_1,x_3,\omega) = H_2^{<}(x_1,x_3,\omega), \tag{7}$$

$$\frac{1}{\epsilon(\omega)}\frac{\partial}{\partial n_+}H_2^{>}(x_1,x_3,\omega) = \frac{\partial}{\partial n_+}H_2^{<}(x_1,x_3,\omega), \tag{8}$$

where $\partial/\partial n_+$, a derivative along the direction normal to the surface at each point, directed from the dielectric into the vacuum, is given by

$$\frac{\partial}{\partial n_+} = \left[1+\left(\frac{d\zeta(x_1)}{dx_1}\right)^2\right]^{-1/2}\left(-\frac{d\zeta}{dx_1}\frac{\partial}{\partial x_1}+\frac{\partial}{\partial x_3}\right). \tag{9}$$

Next, by applying Green's theorem one can, after some algebra, obtain a set of integral equations involving the Fourier amplitudes of the fields at the vacuum-metal interface. Thus, the dispersion relations of the SPP modes can be found by solving the equations

$$\sum_{n=-\infty}^{\infty} I_{m-n}^{(m)}(k\omega)\left[\frac{(\omega/c)^2-k_mk_n}{\alpha_m(k\omega)}H_n(k\omega)+L_n(k\omega)\right]=0, \tag{10}$$

$$\sum_{n=-\infty}^{\infty} J_{m-n}^{(m)}(k\omega)\left[\frac{\epsilon(\omega)(\omega/c)^2-k_mk_n}{\epsilon(\omega)\beta_m(k\omega)}H_n(k\omega)-L_n(k\omega)\right]=0, \tag{11}$$

with

$$k_m = k+2\pi m/a, \tag{12}$$

$$\alpha_m(k\omega) = \begin{cases} [k_m^2-(\omega/c)^2]^{1/2}, & k_m^2>(\omega/c)^2, \\ -i[(\omega/c)^2-k_m^2]^{1/2}, & k_m^2<(\omega/c)^2, \end{cases} \tag{13}$$

and

$$\beta_m(k\omega) = [k_m^2-\epsilon(\omega)(\omega/c)^2]^{1/2}, \tag{14}$$

where m is an integer.

In Eqs. (10) and (11) $H(x_1,\omega)$ and $L(x_1,\omega)$ are given by

$$H(x_1,\omega) = \sum_{n=-\infty}^{\infty}\exp(ik_nx_1)H_n(k,\omega), \tag{15}$$

$$L(x_1,\omega) = \sum_{n=-\infty}^{\infty}\exp(ik_nx_1)L_n(k,\omega). \tag{16}$$

These are related to the tangent field components at the vacuum-dielectric interface by

$$H(x_1,\omega) = H_2^{>}(x_1,x_3,\omega), \tag{17}$$

$$L(x_1,\omega) = -\left[1+\left(\frac{d\zeta(x_1)}{dx_1}\right)^2\right]^{1/2}\frac{\partial}{\partial n_+}H_2^{>}(x_1,x_3,\omega), \tag{18}$$

at the position $x_3=\zeta(x_1)$ The kernel functions $I_l^{(m)}(k\omega)$ and $J_l^{(m)}(k\omega)$ are given by

$$I_l^{(m)}(k\omega) = (1/a)\int_{-a/2}^{a/2}dx_1\exp(-i2\pi x_1l/a)\exp[-\alpha_m(k\omega)\zeta(x_1)], \tag{19}$$

$$J_l^{(m)}(k\omega) = (1/a)\int_{-a/2}^{a/2}dx_1\exp(-i2\pi x_1l/a)\exp[\beta_m(k\omega)\zeta(x_1)]. \tag{20}$$

These functions contain all the information pertinent to the specific shape of the surface and the integrals are calculated in the unit cell interval. The quasiperiodic aspect of the unit cell can be explicitly written into these functions. Similar kernel functions are found in the formalism used in the unretarded regime.

Now we write down the kernel functions in two steps: first by calculating the integrals in Eqs. (19) and (20) for a single ridge, centered at the origin. Next, by introducing suitable changes of variables to the resulting expression we can find the terms associated with the remaining ridges in the unit cell. These changes of variables cause the appearance of exponential factors, which are found to depend on the distance to the origin of the different ridges. Finally, by grouping the exponential factors, the kernel functions can be written as

$$I_l^{(m)}(k\omega) = f_l^a M_l^a(k\omega) + f_l^b M_l^b(k\omega), \tag{21}$$

$$J_l^{(m)}(k\omega) = f_l^a N_l^a(k\omega) + f_l^b N_l^b(k\omega), \tag{22}$$

where $M_l^c(k\omega)$ and $N_l^c(k\omega)$ are identical to Eqs. (19) and (20), respectively, provided we replace a in the integration's limits by L_c, with $c=a, b$. The functions f_l^a and f_l^b arise due to the changes of variables and thus contain the information concerning the positions of each A or B type ridge in the unit cell. Consequently, both functions depend on the particular type of sequence considered, as well as on the sequence term used. The information concerning the shape of the individual ridges is encoded in the functions given by $M_l^c(k\omega)$ and $N_l^c(k\omega)$. The dispersion relations of the SPP modes can be numerically calculated by truncating the summations in Eqs. (10) and (11), writing the resulting expressions in matrix form, and equating the determinant of the coefficients to zero. The convergence of the results will depend on the number of terms retained in the summations, which in turn corresponds to the dimension of the determinant to be calculated. The density of modes is obtained by using the expression[23]

$$\sigma(\omega) = \sum_n \sum_k \delta(\omega - \omega_k), \tag{23}$$

where the first summation on the right-hand side runs over all frequency branches, while the second summation runs through the wave vectors of the first Brillouin zone.

IV. NUMERICAL RESULTS

By using the formalism presented in the previous sections, we now intend to obtain numerical results for the spectra of SPP propagating on the surface of a medium with a dielectric function of the free-electron type, i.e.,

$$\epsilon(\omega) = 1 - \omega_p^2/\omega^2, \tag{24}$$

where ω_p is the plasma frequency of the conduction electrons in the metal. From now on, for simplicity, we will consider $L_a=L_b=L$.

Figure 2 shows the dispersion relations of SPP modes on surfaces created using $p=q=1$ (i.e., the ordinary Fibonacci sequence). We have plotted the reduced frequency $\Omega = \omega/\omega_p$ (in units of the plasma frequency ω_p of the active medium) as a function of the dimensionless wave vector $\xi = ka/\pi$. Here the light line is defined considering $\omega_p a/c=1$ and results were calculated using $A_a/L=0.07$ and $A_b/L=0.03$.

We consider a propagation regime where the SPP are not damped by radiative processes. Specifically, the surface profiles considered here were all *periodic* and extended from $-\infty$ to $+\infty$, with the Fibonacci sequences being expressed in the unit cell. For a periodic surface, the condition for coupling between the SPP modes and the electromagnetic waves is given by $k_{\mathrm{SPP}}=(\omega/c)\sin\theta \pm n|\vec{G}|$, where θ is the angle of incidence and n is an integer (see, e.g., Ref. 24). This condition, which corresponds to $k=(\omega/c)\sin\theta \pm n(2\pi/a)$ in the notation of Sec. III, cannot be satisfied by the wave vectors and profiles considered in this work. Therefore, only real values of α_m will appear in Eq. (13), and the frequencies obtained are always real, in contrast with the results for the radiative region, which would give complex frequencies, with their imaginary part giving the inverse lifetime of the SPP mode. A detailed discussion of this behavior can be found in Refs. 18 and 23.

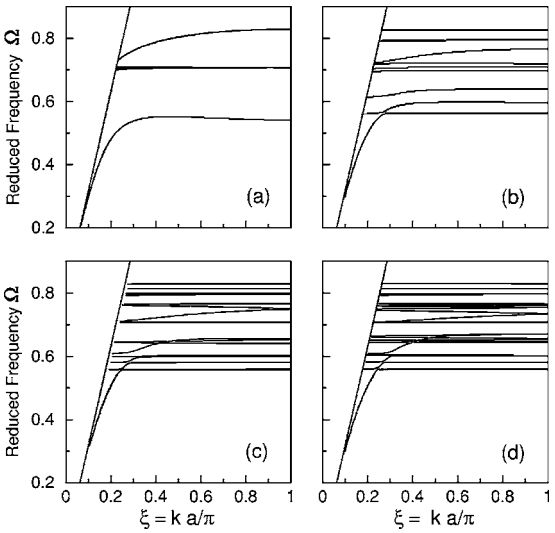

FIG. 2. Dispersion relations for surface plasmon-polariton modes propagating along quasiperiodic surfaces. We have plotted the reduced frequency $\Omega=\omega/\omega_p$ versus the dimensionless wave vector $\xi=ka/\pi$. The results were obtained using the golden mean ratio $p=q=1$, corresponding to the ordinary Fibonacci sequence, for (a) $S_1(F_1=1)$; (b) $S_3(F_3=3)$; (c) $S_5(F_5=8)$; (d) $S_7(F_7=21)$. The other physical parameters are given in the main text.

Therefore, since we are interested in non-radiating modes, the numerical calculation was restricted to the region on the right side of the light line, as seen in the figure. The convergence of the numerically calculated eigenvalues of Eqs. (10) and (11) is dependent on the length of the unit cells, as well as on the magnitude of the frequencies, with the modes closer to the flat surface plasmon frequency $\omega_p/\sqrt{2}$ having a slower convergence than the remaining modes. For example, three-figure convergent results were obtained for matrices with dimension $N=70$ for $L=8a$, whereas for $L=34a$, matrices with dimension $N=190$ were used. In the present case, for small wave vectors ($\xi<0.2$) and low frequencies ($\Omega<0.55$) the SPP dispersion is not noticeably affected by the changes on the surface, for the physical parameters used here. That behavior was expected, since the long-wavelength SPP modes are less sensitive to the shape of the surface. For higher frequencies, the results display a rich behavior, with the appearance of extra frequency branches and several gaps as the system approaches a quasiperiodic surface. Figure 2(a), corresponding to the first Fibonacci sequence, shows the well-known results for a sinusoidal periodic grating.[18] The SPP profiles in Figs. 2(b)–2(d) depict the results for surfaces with unit cells corresponding to increasing terms in the Fibonacci sequence. As the sequence generation increases, one can see the formation of SPP quasibands, with SPP branches separated by narrow frequency gaps. The new SPP branches show little or no dispersion and are roughly

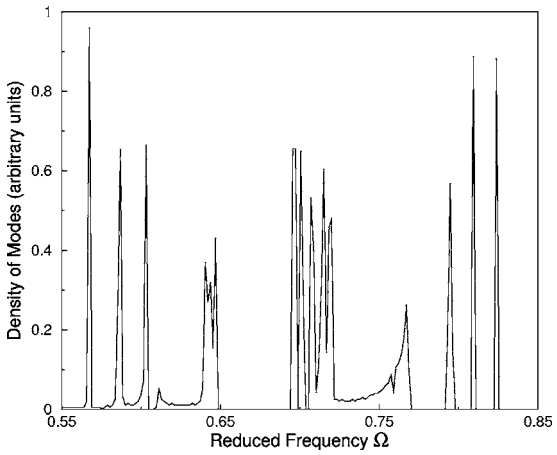

FIG. 3. Density of modes, as a function of the reduced frequency $\Omega=\omega/\omega_p$, for surface polaritons propagating along a quasiperiodic surface created with the fourth generation of the golden mean sequence, considering the size of the quasiperiodic unit cell a equal to $5L$.

symmetrically distributed around $\omega_p/\sqrt{2}$. For the region $0.55<\Omega<0.7$, the graphs show the appearance of mode repulsion and mode crossing effects, arising due to the mixing between propagating and quasilocalized modes. As one approaches the Brillouin zone edge, the results tend to match the spectra calculated in the nonretarded limit.[13]

The results in Fig. 3 show the density of SPP modes for a surface with $p=q=1$ and $A_a/L=0.07$ and $A_b/L=0.03$ plotted against the reduced frequency $\Omega=\omega/\omega_p$. The graph was obtained using Eq. (23) for the S_4 term in the Fibonacci sequence. The results in this figure can be grouped into three different regions: a low-frequency region $(0.56<\Omega<0.65)$, with bands containing peaks separated by narrow gaps; a central region $(0.68<\Omega<0.77)$, containing a broad band with several central peaks, and a high-frequency region $(0.79<\Omega<0.83)$, with well defined peaks separated by wider gaps. The low-frequency region arises due to the mixing between propagating and quasilocalized modes, as can be seen in the dispersion relations. The peaks in the central region lie around the frequency value of SPP modes of a flat surface $(\omega_p/\sqrt{2})$ and are also found in the periodic case. The results show that the frequency band in the central region persists as the sequence generation is increased, apart from the appearance of several narrow gaps, which indicates that this behavior can be interpreted as a consequence of the presence of propagating SPP modes in that frequency range. In contrast, the narrow peaks in the high-frequency region arise due to the absence of mixing with propagating modes. The number of these peaks is dependent on the specific sequence generation and their distribution in the spectrum is strongly dependent on the sequence used.

The fractal aspect of the dispersion can be seen as one plots the normalized integrated density of modes, as a function of the reduced frequency $\Omega=\omega/\omega_p$, as shown in Fig. 4. In this case, the two graphs present results obtained in the high-frequency region for $p=q=1$, $A_a/L=0.07$, and $A_b/L=0.03$, with unit cells corresponding to (a) fourth Fibonacci generation S_4, (b) fifth Fibonacci generation S_5, (c) sixth Fibonacci generation S_6, and (d) seventh Fibonacci generation S_7. The graphs clearly show an emerging self-similar pattern as the sequence generation increases, with the number of modes approaching a devil's staircase function. This behavior is consistent with results calculated for other quasiperiodic multilayer structures.

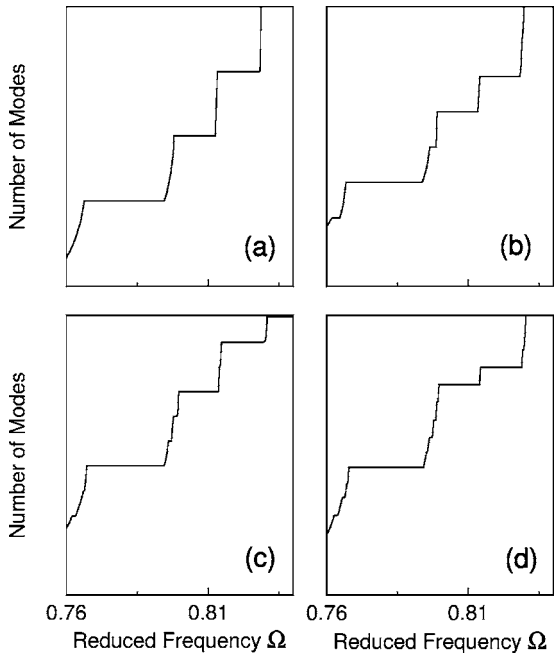

FIG. 4. Normalized integrated density of modes as a function of the reduced frequency $\Omega=\omega/\omega_p$ for retarded surface plasmon-polariton modes propagating along quasiperiodic surfaces with $p=q=1$, $A_a/L=0.07$, $A_b/L=0.03$ and unit cells corresponding to following Fibonacci generations: (a) S_4, (b) S_5, (c) S_6, and (d) S_7.

Figure 5 shows the dispersion relations $\Omega=\omega/\omega_p$ versus $\xi=ka/\pi$ of SPP modes on surfaces created using the silver mean $(p=2,\ q=1)$, with $A_a/L=0.07$ and $A_b/L=0.03$ for (a) the $S_3(a=7L)$ and (b) the $S_4(a=17L)$ Fibonacci generation. As in the previous case, the calculations were performed in the region on the right of the light line. The qualitative aspect of the results is similar to the golden mean case, with the

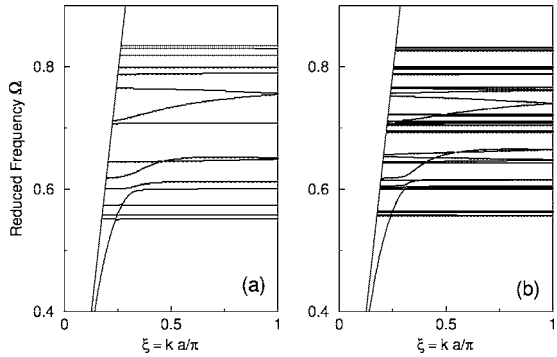

FIG. 5. Dispersion relation of surface plasmon polaritons of quasiperiodic surfaces generated by the silver mean sequence, with $A_a/L=0.07$, $A_b/L=0.03$ and unit cells corresponding to (a) S_3 and (b) S_4. We have plotted the reduced frequency $\Omega=\omega/\omega_p$ versus the dimensionless wave vector $\xi=ka/\pi$.

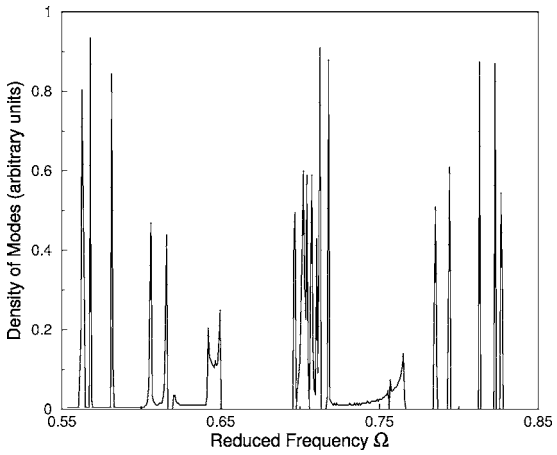

FIG. 6. Density of surface plasmon-polaritons modes plotted versus the reduced frequency $\Omega=\omega/\omega_p$ of a quasiperiodic surface generated given by the silver mean sequence, with $A_a/L=0.07$, $A_b/L=0.03$, and unit cells corresponding to the S_3 sequence generation, considering the size of the quasiperiodic unit cell a equal to $7L$.

SPP modes occurring in the frequency interval as in the previous case. This is a consequence of the fact that in both cases we have used the same ratio for the A and B ridges. Moreover, the propagating mode dispersion is found to be similar to the previous case. On the other hand, the number of dispersionless branches, as well as their distribution in the spectrum, is quite distinct from the golden mean case.

Figure 6 shows the density of modes of the silver mean grating, for the S_3 generation, plotted versus the reduced frequency $\Omega=\omega/\omega_p$. As in the previous results, the spectrum can be separated into three frequency intervals, with a wide band in the central region. The central band is also found to persist as the sequence generation is increased. Moreover, by comparing this figure with the results of the previous case, we find that the central frequency band is only weakly sensitive to the particular sequence used, which indicates that the propagating SPP modes of these structures are less strongly affected by the quasiperiodic aspect of the system. The figure also shows that, for the silver mean, the mode mixing effect at low frequencies is weaker than in the golden mean case, causing the appearance of narrow peaks at low frequencies.

For completeness, we have shown in Fig. 7 the dispersion relation of SPP modes in the nickel mean case ($p=1$, $q=3$), for the S_4 generation ($a=19L$). As in the other cases, the graph shows several dispersionless modes distributed along the $0.55<\Omega<0.84$ interval. On the other hand, in contrast with the results for the golden and silver mean, the figure shows several wider bands both in the low-frequency and in the high-frequency regions. (See Fig. 8.)

V. CONCLUSIONS

We investigated the spectra of surface plasmon-polaritons propagating on interfaces that display deterministic disorder along one direction. The shape of the surfaces was defined

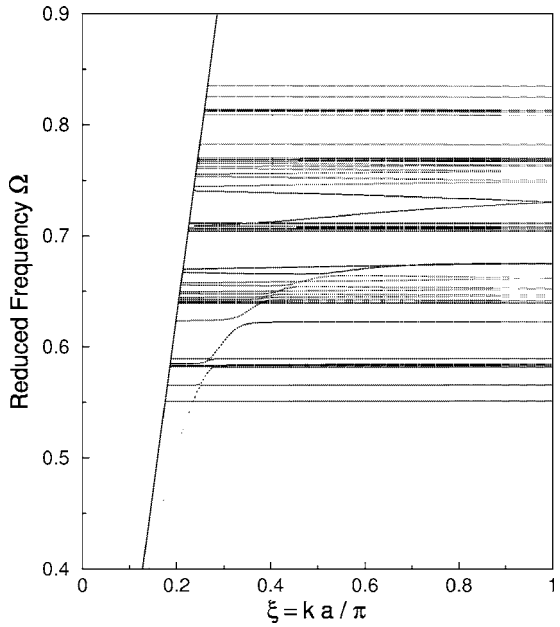

FIG. 7. Dispersion relation of surface plasmon-polariton modes of a quasiperiodic surface generated by the nickel mean, with $A_a/L=0.07$, $A_b/L=0.03$, and unit cell corresponding to the S_4 sequence generation, considering the size of the quasiperiodic unit cell a equal to $19L$.

according to substitutional rules that gave the system a quasiperiodic profile, in analogy with previous studies of quasiperiodic multilayer systems. This model allows the use of an integral method previously developed for the study of surface electromagnetic modes on periodically corrugated inter-

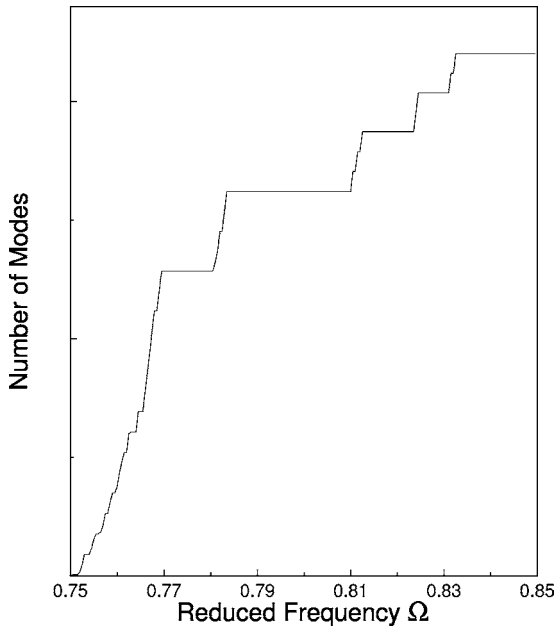

FIG. 8. Normalized integrated density of modes of surface polaritons in quasiperiodic surfaces given by the nickel mean sequence, with $A_a/L=0.07$, $A_b/L=0.03$, and unit cell corresponding to S_5, considering the size of the quasiperiodic unit cell a equal to $40L$.

faces. The results were obtained for interfaces defined by substitutional rules corresponding to the golden mean rule, as well as the silver and nickel means (generalized Fibonacci sequences). The results show the influence of a quasiperiodic interface on the propagation of surface electromagnetic modes. We have found that, for increasing sequence generations, the SPP dispersions show a large number of gaps and dispersionless frequency branches, as well as dispersive branches that depend on the aspect ratio of the surface, but are only weakly influenced by the particular quasiperiodic sequences that describe the surface. Moreover, all the spectra have a fractal characteristic, which is a signature of the excitations propagating in quasiperiodic structures. This fractal aspect of the spectra has been previously predicted for multilayer structures and for nonretarded surface plasmons in quasiperiodic gratings.

Nowadays there is a great interest in the study of SPP modes in patterned surfaces, especially due to recent experimental results that show an extraordinary transmission of light through a metallic slab containing subwavelength holes. There is also interest in possible applications of SPP in data storage, light generation, microscopy, and biophotonics. These applications involve the tailoring of the SPP spectra in order to modify the field intensity at the surfaces. In fact, this modification has been recently applied to enhance the light-emission efficiency of light-emitting diodes.[25]

The results presented here correspond to gratings where the unit cells have lengths a up to $40L$. As one approaches a true quasiperiodic surface, the lengths of the cells grow, and that in turn decreases the wave vector range of the undamped region. Therefore, for cells corresponding to higher-order sequences, the radiative damping will become an important factor in the calculations. On the other hand, modern patterning techniques have been used to create surface structures with dimensions of the order of 10 nm.[26] For silver as the active medium ($\hbar\omega_p = 3.78$ eV), the dispersion results obtained correspond to gratings with periods of 330 nm, which indicates that existing technologies may be capable of creating surfaces that display some of the behaviors described here.

Despite the fact that only the nonradiative region of the spectrum was considered in this work, it seems clear that the quasiperiodic aspect of the surface should also have a strong influence on the light-SPP interaction. The properties of these surfaces can allow the observation of phenomena previously associated with quasiperiodic layered structures, which by themselves have been attracting a great deal of interest in recent years.[14] Furthermore, the existence of flat SPP branches for the surfaces studied means that SPP modes in the radiative regime could be excited by light that is incident over a wide range of angles, making them good candidates for frequency-selective surfaces.[7] An experimental investigation of these surfaces could be carried out by means of prism couplers in an ATR measurement, as used before to probe SPP in a periodic surface.[10] Future studies should extend the investigation to the radiative regime, including a study of the light scattering properties of quasiperiodic surfaces.

ACKNOWLEDGMENTS

The authors acknowledge the partial financial support of CNPq, MCT-NanoSemiMat, CAPES-Procad, and FINEP-CTInfra (Brazilian Research Agencies).

[1] G. Van Simaeys, S. Coen, M. Haelterman, and S. Trillo, Phys. Rev. Lett. **92**, 223902 (2004).
[2] K. Nozaki and T. Baba, Appl. Phys. Lett. **84**, 4875 (2004).
[3] D. Gerard, L. Salomon, F. de Fornel, and A. V. Zayats, Phys. Rev. B **69**, 113405 (2004).
[4] T. W. Ebbesen, H. J. Lezec, H. F. Ghaemi, T. Thio, and P. A. Wolff, Nature (London) **391**, 667 (1998).
[5] H. J. Lezec, A. Degiron, E. Devaux, R. A. Linke, L. Martin-Moreno, F. J. Garcia-Vidal, and T. W. Ebbesen, Science **297**, 820 (2002).
[6] D. T. Crouse and Y. H. Lo, J. Appl. Phys. **95**, 4163 (2004).
[7] W. L. Barnes, A. Dereux, and T. W. Ebbesen, Nature (London) **424**, 824 (2003).
[8] A. A. Maradudin, I. Simonsen, T. A. Leskova, and E. R. Méndez, Physica B **296**, 85 (2001).
[9] S. I. Bozhevolnyi, J. Erland, K. Leosson, P. M. W. Skovgaard, and J. M. Hvam, Phys. Rev. Lett. **86**, 3008 (2001).
[10] S. C. Kitson, W. L. Barnes, and J. R. Sambles, Phys. Rev. Lett. **77**, 2670 (1996).
[11] M. Moskovits, Rev. Mod. Phys. **57**, 783 (1985).
[12] S. I. Bozhevolnyi, J. Beermann, and V. Coello, Phys. Rev. Lett. **90**, 197403 (2003).
[13] J. M. Pereira, Jr., G. A. Farias, and R. N. Costa Filho, Eur. Phys. J. B **36**, 137 (2003).
[14] E. L. Albuquerque and M. G. Cottam, Phys. Rep. **376**, 225 (2003).
[15] R. Merlin, K. Bajema, R. Clarke, F.-Y. Juang, and P. K. Bhattacharya, Phys. Rev. Lett. **55**, 1768 (1985).
[16] P. W. Mauriz, M. S. Vasconcelos, and E. L. Albuquerque, Physica A **329**, 101 (2003).
[17] U. Grimm and M. Baake, in *The Mathematics of Long-Range Aperiodic Order*, edited by R. V. Moody (Kluwer, Dordrecht, 1997).
[18] B. Laks, D. L. Mills, and A. A. Maradudin, Phys. Rev. B **23**, 4965 (1981).
[19] F. Toigo, A. Marvin, V. Celli, and N. R. Hill, Phys. Rev. B **15**, 5618 (1977).
[20] N. E. Glass and A. A. Maradudin, Phys. Rev. B **24**, 595 (1981).
[21] N. E. Glass, A. A. Maradudin, and V. Celli, Phys. Rev. B **26**, 5357 (1982).
[22] S. Dutta Gupta, G. V. Varada, and G. S. Agarwal, Phys. Rev. B **36**, 6331 (1987).
[23] M. Kretschmann and A. A. Maradudin, Phys. Rev. B **66**, 245408 (2002).
[24] H. Raether, *Surface Plasmons* (Springer-Verlag, Heidelberg, 1988).
[25] K. Okamoto, I. Niki, A. Shvartser, Y. Narukawa, T. Mukai, and A. Scherer, Nat. Mater. **3**, 601 (2004).
[26] N. A. Melosh, A. Boukai, F. Diana, B. Gerardot, A. Badolato, P. M. Petroff, and J. R. Heath, Science **300**, 112 (2003).